Manuscript ID: 242
DOI: 10.18462/iir.icr.2019.0242

High temperature heat pump using HFO and HCFO refrigerants – system design and experimental results

Cordin ARPAGAUS[(a)], Ralph KUSTER[(a)], Manuel PRINZING[(a)], Frédéric BLESS[(a)], Michael UHLMANN[(a)], Elias BÜCHEL[(a)], Stefan FREI[(a)], Jürg SCHIFFMANN[(b)], Stefan S. BERTSCH[(a)]

[(a)] NTB University of Applied Sciences of Technology Buchs, Institute for Energy Systems, Werdenbergstrasse 4, 9471 Buchs, Switzerland, cordin.arpagaus@ntb.ch
[(b)] Ecole Polytechnique Fédérale de Lausanne, Laboratory for Applied Mechanical Design, Rue de la Maladière 71b, 2002 Neuchâtel, Switzerland

ABSTRACT

High temperature heat pumps (HTHP) with heat sink temperatures of 100 to 160 °C will increasingly become commercialized in the coming years, especially for industrial drying, sterilization and evaporation processes. In particular, the HFO R1336mzz(Z) and the HCFOs R1233zd(E) & R1224yd(Z) are low GWP (< 10) replacement refrigerants for R245fa and R365mfc. This study examines the experimental performance of R1336mzz(Z) and R1233zd(E) in a laboratory HTHP with 5 to 10 kW heating capacity. The developed heat pump is single-stage, operates with a variable speed piston compressor, and contains a continuously adjustable internal heat exchanger (IHX) for superheating control. The performance data were measured at 30, 50, and 70 K temperature lift (40 to 80°C heat source, 80 to 150°C heat sink). At W60/W110 the experimental results with R1233zd(E) showed a COP of 2.8 (basic cycle) and 3.1 with IHX integration (+15%). For R1336mzz(Z) a COP of 2.4 and 3.0 was reached (+24%). At higher temperatures tested, the deviations between the measured COP with R1336mzz(Z) and R1233zd(E) were within the measurement uncertainty. Moreover, R1336mzz(Z) achieves potentially higher condensing temperatures due to its higher critical temperature. By increasing the heat sink temperature glide from 5 to 30 K, a further 15% COP increase was achieved.
Keywords: High temperature heat pump, HFO, HCFO, R1336mzz(Z), R1233zd(E), R1224yd(Z), efficiency, COP

1. INTRODUCTION

High temperature heat pumps (HTHP) with heat sink temperatures in the range of 100 to 160 °C will become increasingly available on the market in the coming years (Arpagaus et al., 2017, 2018b, 2018c). Potential applications for HTHP are found in various industrial processes such as drying, sterilization, steam generation, papermaking, food preparation, and heat recovery. Waste heat at a low temperature can be efficiently converted into usable process heat. The replacement of fuel driven steam boilers by heat pumps would be a significant contribution (Nilsson et al., 2017). In addition, multi-temperature heat pumps using multiple heat sources and heat sinks with different temperature levels are potential systems to further increase system efficiency (Arpagaus et al., 2016).

There is a high level of research activity in the field of HTHP technology development at the international level. The main research objectives are the extension of heat source and sink temperatures to higher values, the improvement of heat pump efficiency, the testing of new environmentally friendly refrigerants, and in particular the scale-up from laboratory to industrial scale. With the stricter F-Gas regulation, only refrigerants with a global waring potential (GWP) of less than 150 may be used in new commercial heat pumps starting from 2022. The greenhouse effective hydrofluorocarbon (HFC) refrigerants R245fa and R365mfc (GWP of 858 and 804) are therefore subject to a "phase-down" (i.e. reduction of production and consumption) in most industrialised countries. Replacement refrigerants are currently being developed and researched. Natural refrigerants such as water (R718) or hydrocarbons (e.g. R600 and R601) are promising environmentally friendly substitutes. However, special heat pump cycles with multi-stage

compression (e.g. vapour recompression) or sophisticated safety measures due to flammability are required, which can increase system costs.

In recent years, various hydrofluoroolefins (HFO) and hydrochlorofluoroolefins (HCFO) have been developed which exhibit very low GWP, are non-combustible and have great potential for use as refrigerants in HTHPs. Table 1 lists some suitable HFO and HCFO refrigerants including their thermodynamic, environmental and safety parameters. R1233zd(E) with a critical temperature of 166.5 °C and a critical pressure of 36.2 bar is available as Solstice®zd from Honeywell or Forane®HTS 1233zd from ARKEMA. Although R1233zd(E) contains chlorine, its ODP is extremely small (0.00034) and the atmospheric lifetime is only 40.4 days (Patten & Wuebbles, 2010). The advantages of R1336mmz(Z) are the higher critical temperature of 171.3°C at a feasible pressure of 29.0 bar. Its safety class is A1, and it has a GWP of 2, an ODP of 0, and an atmospheric life of only 22 days (Myhre et al., 2013). Chemours commercialized R1336mzz(Z) under the brand Opteon™MZ. Polyolester oil (POE) with high viscosity is recommended as lubricant, as it is fully miscible over wide ranges of temperatures and compositions (Kontomaris, 2014a, 2014b). R1224yd(Z) is another non-combustible (A1) HCFO refrigerant designed for use in heat pumps for waste heat recovery. AGC Chemicals (Asahi Glass) markets the refrigerant as Amolea®1224yd (AGC Chemicals, 2017). With an ODP of almost zero (0.00012, atmospheric lifetime of 21 days) and a GWP < 1, it has a low environmental impact. The physical properties are close to R245fa and R1233zd(E). Relatively little information is available on R1234ze(Z), which has a critical temperature of 150.1°C and a critical pressure of 35.3 bar (Kondou and Koyama, 2015). Its GWP is < 1 (Myhre et al., 2013) and its flammability is rated with A2L (Fukuda et al., 2014). R1234ze(Z) is assessed as a promising “drop-in” substitute for R114 in HTHP applications (Brown et al., 2009).

Table 1. Properties of HFO and HCFO refrigerants suitable for HTHP (bold: refrigerants tested in this study, HFC refrigerants R365mfc and R245fa for comparison)

Refrigerant	Brand (manufacturer)	T_{crit} (°C)	p_{crit} (bar)	ODP (-)	GWP_{100} (-)	Lifetime (days)	SG	NBP (°C)
R1336mzz(Z)	**Opteon™MZ (Chemours)**	**171.3**	**29.0**	**0**	**2**	**22**	**A1**	**33.4**
R1234ze(Z)	not yet available	150.1	35.3	0	<1	18	A2L	9.8
R1233zd(E)	**Solstice®zd (Honeywell)** Forane®HTS 1233zd (ARKEMA)	**166.5**	**36.2**	**0.00034**	**1**	**40.4**	**A1**	**18.0**
R1224yd(Z)	AMOLEA®1224yd (AGC Chemicals)	155.5	33.3	0.00012	<1	21	A1	14.0
R365mfc	Solkane®365mfc (Solvay)	186.9	32.7	0	804	8.7 years	A2	40.2
R245fa	Genetron®245fa (Honeywell)	154.0	36.5	0	858	7.7 years	B1	14.9

Table 2 shows an overview of experimental studies published in the literature on HTHPs with R1336mzz(Z) and R1233zd(E). The heating capacities range from about 1.8 to 12 kW for the laboratory prototypes (Arpagaus et al., 2018a; Fleckl et al., 2015; Fukuda et al., 2014; Helminger et al., 2016). The commercial HeatBooster S4 from Viking Heat Engines (2018) represents the industrial benchmark with heat sink outlet temperatures of up to 160 °C using R1336mzz(Z) and up to 200 kW heating capacity (Nilsson et al., 2017; Viking Heat Engines, 2018). Four piston compressors are connected in parallel to increase the capacity. Helminger et al. (2016) reported a highest heat sink outlet temperature of 156.3 °C (condensation at 160°C) in a single-stage laboratory HTHP with IHX with a coefficient of performance (COP) of 2.67 and a temperature lift of 47.4 K. In a previous study, Fleckl et al. (2015) reached 150°C with a basic cycle at a COP of 2.4 and a temperature lift of 70 K.

Table 2. Published experimental research studies testing HFO refrigerants in HTHP systems

Organisation partners	Refrigerant	Heat sink/ source T (°C)	Heating capacity (kW)	Com-pressor	Cycle	References
AIT, Chemours, Bitzer	R1336mzz(Z)	75-160/30-110	12	Piston	1-stage with IHX	(Helminger et al., 2016)
Viking Heating Engines AS	R1336mzz(Z)	80-160/35-110	75-200	Piston (4 parallel)	1-stage with IHX	(Nilsson et al., 2017)
NTB Buchs,	R1233zd(E)	70-150/40-80	3-10	Piston	1-stage with	(Arpagaus et

In our previous study, first experimental results of a single-stage laboratory HTHP system using R1233zd(E) (Solstice®zd from Honeywell) have been presented. At the reference point conditions (W60/W110) a COP of 2.43 was achieved (Arpagaus et al., 2018a). The system was capable of testing heat source temperatures of 40 to 80 °C and sink temperatures of 80 to 150 °C.
This paper continues these studies and examines the performance of R1336mzz(Z) (Opteon™MZ from Chemours) and R1233zd(E) (Solstice®zd from Honeywell) in the same laboratory HTHP plant after improved insulation of some components (e.g. oil separator, liquid receiver, and suction line accumulator) with Armaflex®HT insulation. The system design with the integration of an IHX into the cycle and the experimental test results of a parameter study are presented and compared with literature data. In particular, the COP is investigated as a function of the temperature lift between the heat source and the heat sink, the temperature glide on the heat sink side and the refrigerant charge.

2. EXPERIMENTAL DESIGN AND TEST PROCEDURE

Figure 1 illustrates the developed HTWP laboratory plant (A) with the schematic diagram (B) and the two pressurized water loops for the heat source and heat sink (C). The HTHP is single-stage and operates with a variable-speed semi-hermetic piston compressor (Bitzer, 2DES-3Y New Ecoline). An integrated temperature sensor prevents overheating of the motor with a switch-off temperature of approx. 110°C. The heat pump contains an IHX for increasing the suction gas temperature (T_1), which ensures dry compression and simultaneously subcools the refrigerant after condensation.
The superheat for controlling the expansion valve (EXV) is measured after the evaporator at state point 6 (before the IHX) and was set to 5 K for all experiments ($\Delta T_{SH} = T(p_5) - T_6$). The liquid subcooling after the condenser was calculated by $\Delta T_{SC} = T(p_3) - T_4$.
The refrigerant mass flow through the IHX is continuously adjustable from 0% to 100% via a 3-way valve (Siemens). A receiver serves as a refrigerant collector after condensation and ensures liquid refrigerant prior to the expansion valve. An oil separator is installed on the high pressure side, which returns the collected oil back to the compressor via a cooling pipe. The heat exchangers are compact plate heat exchangers with low pressure drops. The heat source inlet temperature ($T_{Source,in}$) can be varied between 40 and 80 °C and the heat sink outlet temperature ($T_{Sink,out}$) between 70 and 150 °C. The heat source circuit simulates potentially available waste heat from an industrial process and includes a controllable electrical heater (Backer ELC, 10 kW), a water pump with adjustable flow rate, and an expansion vessel with safety valve. The heat sink represents a potential HTHP application (e.g. steam generation or drying process) and includes a water cooler to dissipate the generated heat to the environment. The electrical heater controls the heat source inlet temperature ($T_{Source,in}$) and a control valve (BELIMO, 2-way zone valve with rotary actuator) at the inlet of the water cooler the heat sink inlet temperature ($T_{Sink,in}$) into the condenser.
The temperatures are measured with calibrated thermocouples (type K, class 1) with an accuracy of ± 0,1 K. Differential temperature measurement is used at the input and output of the heat pump (ΔT_{Sink}, ΔT_{Source}). A Coriolis flow meter (E+H, Promass F300) measures the water mass flow in the heat sink circuit with an accuracy of ± 0.05 %. A power transmitter (Infratek, ITL-101) measures the electrical power consumption of the compressor with an accuracy of ± 3 %. A CompactRIO® cRIO-9022 from National Instruments in combination with LabVIEW™2017myRio is used for data acquisition and control. All components are commercially available without modifications.

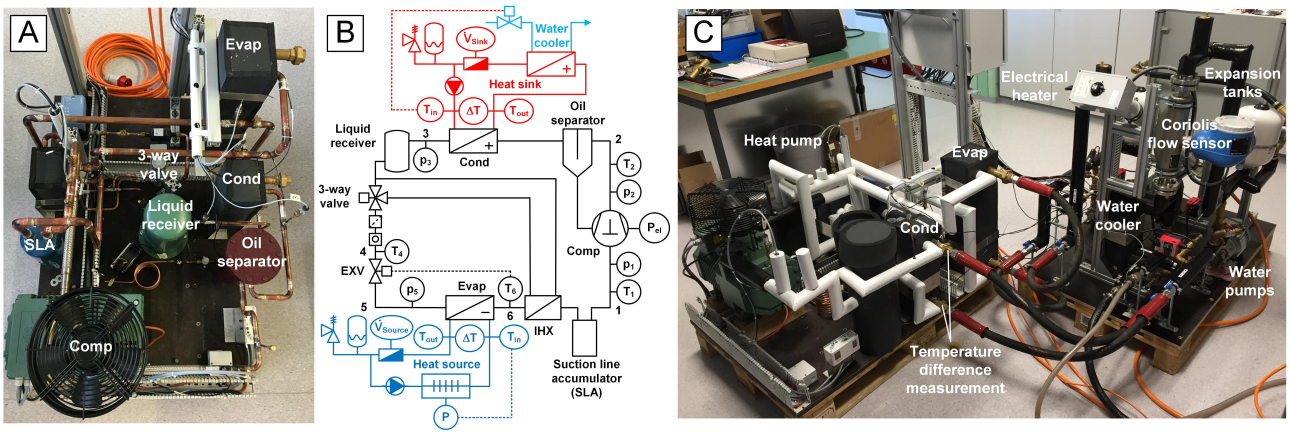

Figure 1: (A) Experimental setup, (B) schematic diagram, and (C) hydraulic loops (heat source and heat sink) of the developed laboratory scale HTHP plant

More details on the components and sensors are described in the paper of Arpagaus et al. (2018a). The filling quantities for the refrigerants R1233zd(E) and R1336mzz(Z) were 4.2 kg and 4.1 kg, respectively. To achieve sufficient lubrication at high operating temperatures, POE oil (Reniso Triton SE170) was selected with a kinematic viscosity of 173 mm^2/s at 40°C (17,6 mm^2/s at 100 °C).

After heating up the HTHP to the desired heat source and heat sink temperatures, the water flow rates in the two hydraulic circuits were adjusted by the pumps to receive constant temperature differences of 3.0 ± 0.1 K at a heat source (ΔT_{Source}) and 5.0 ± 0.1 K at the heat sink (ΔT_{Sink}). Mean values of at least 5 minutes under stationary conditions were used for the data analysis. The heating COP was determined from the measured heating capacity ($\dot{Q}_{Sink}$) and the electrical power consumption of the compressor (P_{el}) according to Eq. (1). The 2nd Law efficiency was determined by Eq. (2). The temperature dependence of the specific heat capacity of water was taken into account.

$$COP_H = \dot{Q}_{Sink}/P_{el} = \left(\dot{m}_{H_2O} \cdot c_{p,H_2O}(T) \cdot \Delta T_{Sink}\right)/P_{el} \qquad \text{Eq. (1)}$$

$$\square_{2nd} = COP_H/COP_{Carnot} \text{ with } COP_{Carnot} = T_{Sink,out}/\left(T_{Sink,out} - T_{Source,in}\right) \qquad \text{Eq. (2)}$$

3. EXPERIMENTAL RESULTS AND DISCUSSION

3.1. Results with R1233zd(E)

The most important measurement results of the parameter study with R1233zd(E) are illustrated in Figure 2 (A) to (F). Figure 2 (A) shows the experimentally measured COP_H of the laboratory plant as a function of the investigated heat sink outlet temperature ($T_{Sink,out}$) at different temperature lifts ($\Delta T_{Lift} = T_{Sink,out} - T_{Source,in}$) from 30 to 70 K. As expected, the COP increased with smaller temperature lift and higher heat sink outlet temperature according to the Carnot relationship (Eq. 2). At the reference point (Ref) W60/W110 (50 K temperature lift) a COP of 2.8 ± 0.2 was measured with the basic cycle. The better insulation of the heat pump compared to the earlier studies by Arpagaus et al. (2018a) led to an increase in efficiency of about 15%. In comparison to the basic cycle, the integration of the IHX into the circuit led to a further COP increase of approx. 15% to 3.1. Since the suction gas superheat is achieved in the IHX and not in the evaporator, the evaporation temperature in the IHX circuit is higher than in the basic cycle. This results in a higher refrigerant density at the compressor inlet and an increased efficiency. The maximum heat sink temperature tested was 150°C, whereby a COP of 2.1 was achieved with a heat source of 80°C (70 K lift). The slightly decreasing COP curve at 70 K lift is the result of the narrower two-phase region for condensation near the critical point and the increasing heat losses ($\dot{Q}_{Loss}$) of the system due to natural convection and radiation of the uninsulated parts (i.e. compressor).

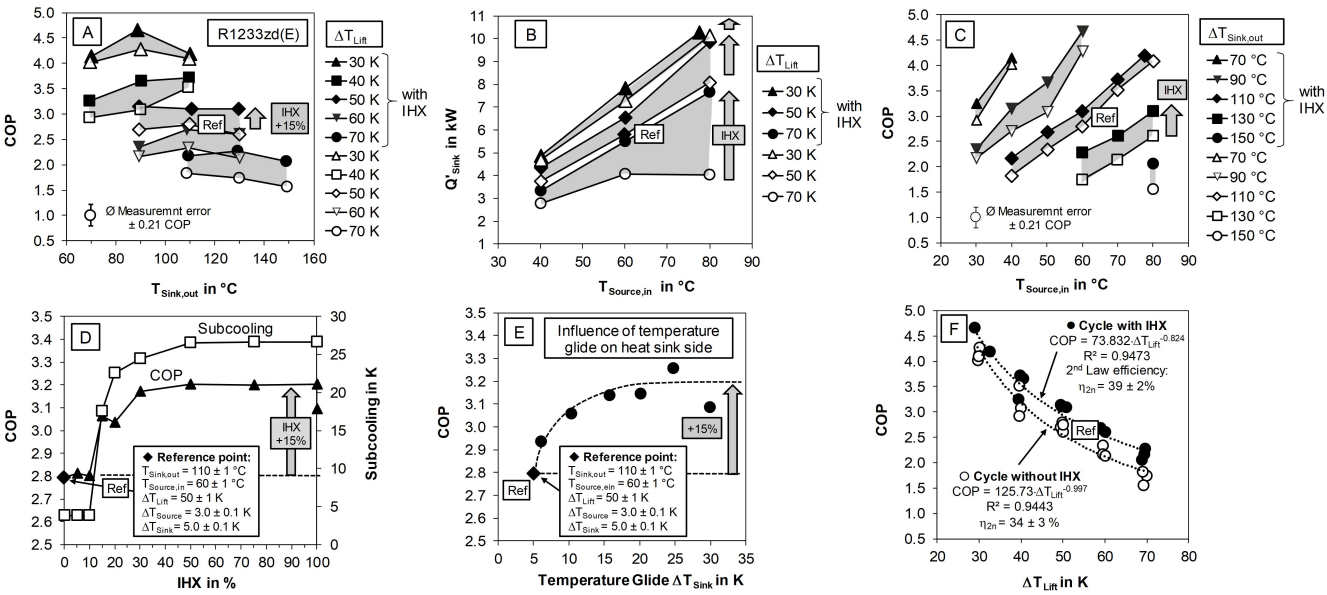

Figure 2: Experimental results with the refrigerant R1233zd(E). (A) Operating map, (B) heating capacity, (C) COP vs. heat source temperature with and without IHX, (D) influence of the IHX on the COP at the reference point (W60/W110), (E) efficiency increase with higher temperature glide on the heat sink side, (F) curve fit of the COP measurement data vs. temperature lift

Heat losses of about 21 ± 7 % could be estimated from the energy balance of the heat pump ($\dot{Q}_{Loss} \approx \dot{Q}_{Source} + P_{el} - \dot{Q}_{Sink}$) leading to a 2nd Law efficiency of about 39 ± 2 % (with IHX in the cycle) (see Figure 2, F). In other words, there is still potential for optimisation in insulation (especially at the compressor) and possibilities for increasing efficiency. For large-scale application, the relative heat losses will be significantly lower due to higher energy density of the heat pump.

Figure 2 (B) illustrates the heating capacity ($\dot{Q}_{Sink}$) as a function of the heat source inlet temperature ($T_{Source,in}$) at constant temperature lifts (ΔT_{Lift}). The heating capacity increased steadily with temperature according to Carnot's relationship (Eq. 2). At Ref conditions, the heating capacity was about 5.8 kW and increased to about 10 kW at W80/W110. At this operating point, the heat pump reached its experimental capacity limits.

Figure 2 (C) provides an overview of the entire operating map of the HTHP with and without IHX at the same experimental temperature conditions. The increase in efficiency with the use of the IHX is evident. For example, the COP at W80/W150 increased from 1.6 to 2.1 or at W60/W110 (Ref) from 2.8 to 3.1. For W80/W130, the suction (T_1) and discharge (T_2) temperatures were 112 °C and 161 °C, respectively, and thus close to the temperature limit of the compressor motor. Excessively high discharge gas temperatures are limited by the compressor switch-off temperature.

Figure 2 (D) shows the influence of the IHX on the COP from 0 to 100 % opening degree of the 3-way valve at the reference point (W60/W110). Compared to the basic heat pump cycle, the suction gas is additionally superheated in the IHX and the liquid refrigerant subcooled. When the IHX is integrated, both the suction gas (T_1) and discharge gas (T_2) temperatures as well as the COP increased due to the higher heating capacity. The COP levelled off with increasing flow through the IHX, indicating a sufficiently large IHX heat exchanger. The integration of the IHX provides additional flexibility in superheat control for future applications with alternative low GWP refrigerants that require high superheat (strongly overhanging two-phase region to the right in the log(p)-h diagram).

The graph in Figure 2 (E) shows the effect of a higher heat sink temperature glide (ΔT_{Sink}) on the COP varied from the Ref conditions as an example of a potential process heating application. With increasing temperature glide from 5 to 30 K (at constant $T_{Source,out}$) the heat transfer in the condenser improves, which led to a 12 % higher heating capacity and approx. 15 % higher COP.

Figure 2 (F) shows the determined COPs of the entire measurement data as a function of the respective temperature lift between heat source and sink. The COP values decrease with higher temperature lift and correspond to a curve with 39 ± 2 % and 34 ± 3 % 2nd Law efficiency (η_{2nd}) for the IHX cycle and the basic cycle, respectively.

3.2. Results with R1366mzz(Z)

The experimental results with R1336mzz(Z) are shown in Figure 3 (A) to (E). Figure 3 (A) presents the system performance as a function of the investigated heat sink outlet temperature ($T_{Sink,out}$) at different temperature lifts (ΔT_{Lift}) from 30 to 70 K. At the reference point (Ref) W60/W110, a COP of 2.4 was achieved with the basic cycle. The integration of the IHX into the circuit significantly increased efficiency across the entire operating map, e.g. up to +47% at W80/130 (50 K temperature lift). This is in line with Helminger et al. (2016) where an efficiency increase of 4 to 10 % and 19 to 47 % at about 20 K and 45 K temperature lift was observed with the integration of an IHX.

Figure 3 (B) shows the heating capacity ($\dot{Q}_{Sink}$) as a function of the heat source inlet temperature ($T_{Source,in}$) at constant temperature lifts (ΔT_{Lift}). The IHX significantly increases the heating capacity compared to the basic cycle, especially for high temperature lifts between heat source and heat sink. The heating capacity under Ref conditions was approx. 3.4 kW and increased to approx. 7.8 kW at W80/W110 with IHX cycle. Overall, the heating capacity of R1336mzz(Z) was about 46 to 76% lower than that of R1233zd(E). This is due to the lower volumetric heating capacity (VHC) of R1336mzz(Z). A larger compressor would be required to achieve similar heating capacities as R1233zd(E). This is in agreement with simulation studies by Arpagaus et al. (2018b), where at 60 °C/130 °C (evaporation/condensation temperatures) VHC values of 1'779 kJ/m^3 and 2'594 kJ/m^3 (+46%) were calculated for R1336mzz(Z) and R1233zd(E), respectively.

Figure 3 (C) shows the operating map without and with IHX in the cycle at the same experimental temperature conditions as in Figure 3 (A). The increase in efficiency with the use of the IHX is evident as in the operating map of R1233zd(E) (see Figure 2, C). For example, at operating point W80/W150 (70 K lift) a COP of 1.8 could be measured.
Figure 3 (D) shows the suction (T_1) and discharge (T_2) temperatures as a function of the heat sink outlet temperature. Overall, the suction temperature in the basic cycle (Δ) was well below the motor shut-off temperature of approx. 110°C (indicated by a grey line). With the IHX cycle, the suction temperature (○) exceeded the motor limit temperature at a heat sink outlet temperature of about 130°C and higher. However, short-term experiments over several minutes were still possible to run, especially at 150°C.
Figure 3 (E) illustrates the influence of refrigerant charge for R1336mzz(Z) on COP under reference conditions with the IHX cycle. With increasing refrigerant charge, the COP reached a plateau and the performance became almost independent of the charge. This result is of practical interest, as the experimental tests were carried out with a charge of 4.1 kg. The liquid receiver (5.6 L volume) ensured liquid refrigerants prior of the expansion valve. In addition, the sight glass in the liquid line between condenser and expansion valve was inspected to be clear (no presence of gas bubbles), as a rough check for sufficient refrigerant charge.
Figure 3 (F) shows the measured COP data of the basic and IHX cycle as a function of the temperature lift. Positive effects on the COP are a small temperature difference between heat source and heat sink. 2nd Law efficiencies of 34 ± 3 % and 29 ± 3 % were obtained, respectively. For comparison, Fleckl et al. (2015) reported values of about 35 to 50 % in a laboratory single-stage heat pump with R1336mzz(Z).

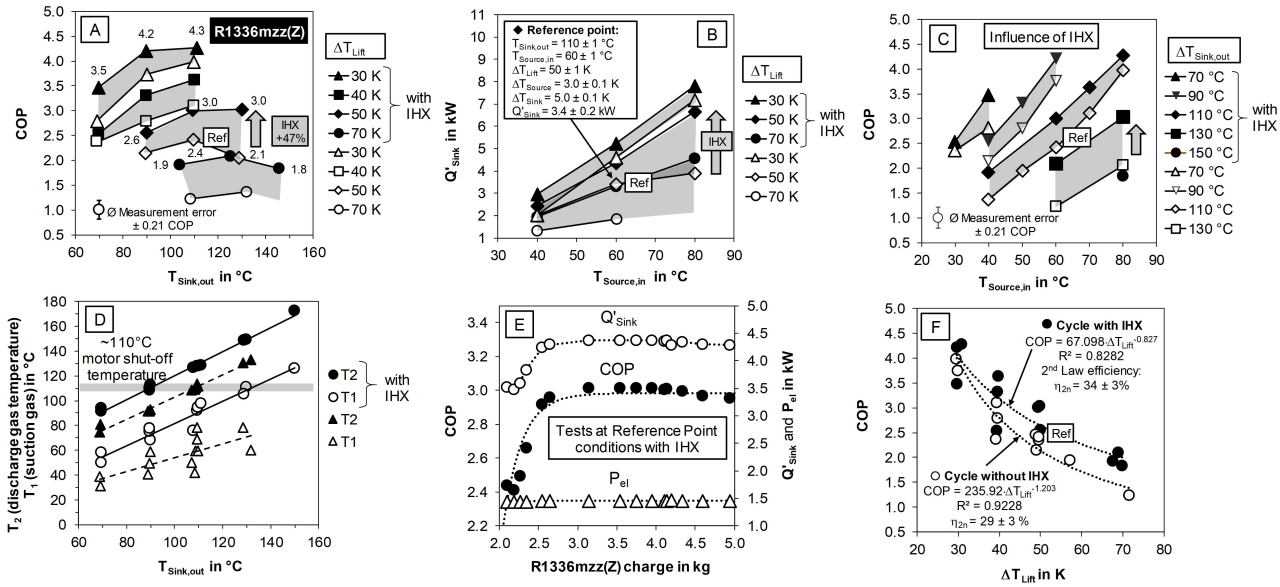

Figure 3: Performance figures with the refrigerant R1336mzz(Z). (A) Operating map, (B) heating capacity, (C) COP vs. heat source temperature with and without IHX, (D) discharge and suction gas temperatures, (E) influence of the refrigerant charge on the COP at the reference point (W60/W110), (F) curve fit of the COP measurement data vs. temperature lift

Figure 4 (A) compares the measured operating maps of the refrigerants R1233zd(E) and R1336mzz(Z) in the HTHP with the IHX cycle at the same temperature conditions (Figure 2 A and Figure 3 A). The comparison indicates that the heat pump was capable of achieving a slightly higher COP with R1233zd(E) than with R1336mzz(Z) at heat sink outlet temperatures of up to about 110°C.
This is attributed to the smaller heating capacity of R1336mzz(Z), which means that the relative heat losses are more significant. Thereafter the deviations are in the measurement uncertainty of the experiments. At higher temperatures, both refrigerants have comparable efficiency. R1336mzz(Z) achieves potentially higher condensing temperatures due to the higher critical temperature of 171.3°C (compared to 166.5 °C of R1233zd(E)). In this study, the maximal tested heat sink temperature was 150 °C.

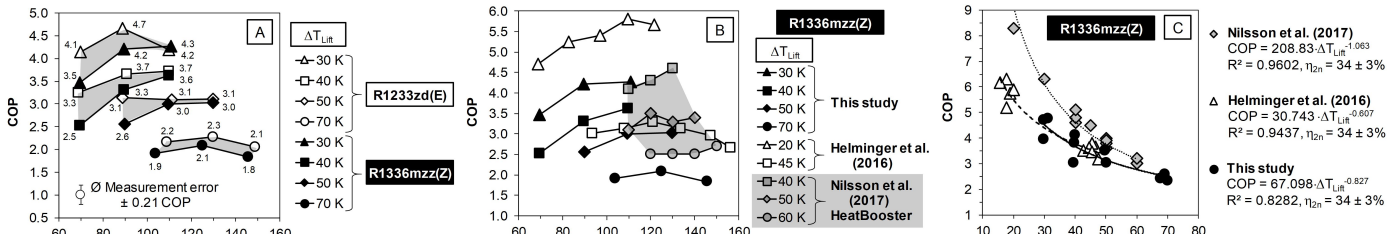

Figure 4: (A) Comparison of the operating maps of (A) R1233zd(E) vs. R1336mzz(Z). (B) and (C) Comparison of the R1336mzz(Z) operating map with literature data from Helminger et al. (2016) (laboratory scale setup) and Nilsson et al. (2017) (HeatBooster from Viking Heating Engines)

Figure 4 (B) and (C) compare the performance map of R1336mzz(Z) at different temperature lifts with literature data from Helminger et al. (2016) and Nilsson et al. (2017). Helminger et al. (2016) reported heat sink temperatures of up to 156.3°C and a COP of almost 2.7 with a temperature lift of about 45 K. The 2nd Law efficiency of the laboratory setup corresponded to 34 ± 3%, thus similar to our study. The commercial HeatBooster technology achieves a higher efficiency with a 2nd Law efficiency of 41 ± 3 %. Even at 60 K temperature lift, a COP of 2.5 is achieved. This increase in performance is partially attributable to a larger temperature glides tested on the heat sink side of 10 and 20 K, compared to 5 K in this study, which leads to an increase in efficiency. In addition, with larger heating power the relative heat losses are smaller.

4. CONCLUSIONS

The operating maps of a laboratory HTHP system with the refrigerants R1233zd(E) and R1336mzz(Z) could be experimentally examined at 40 to 80 °C heat source and 70 to 150 °C heat sink temperatures. The integration of an IHX in the heat pump cycle significantly increased the efficiency and the heating capacity over the entire operating map. At W60/W110 (reference point) a heating COP of 2.8 was achieved for R1233zd(E) with the basic cycle and 3.1 with IHX integration (+15%). For R1336mzz(Z) a COP of 2.4 was reached with the basic and 3.0 with the IHX cycle (+24%). Up to a heat sink outlet temperature of about 110°C, R1233zd(E) delivered a slightly higher COP than R1336mzz(Z) due to higher heating capacity and smaller relative heat losses at the same temperature conditions. At the higher temperatures tested, the deviations between the measured COP with R1336mzz(Z) and R1233zd(E) were within the measurement uncertainty (± 0.21 COP). R1233zd(E) provided a heating capacity on 5.8 kW at the reference point and approx. 10 kW at W80/W110, which corresponded to the capacity limit of the laboratory plant. With R1336mzz(Z) a maximum heating capacity of 7.8 kW could be achieved. For R1336mzz(Z) a larger compressor would be required to achieve similar heating capacities as R1233zd(E). Moreover, R1336mzz(Z) achieves potentially higher condensing temperatures due to its higher critical temperature of 171.3 °C. An increase in the temperature glide on the heat sink side from 5 to 30 K raised the COP by another +15%, which is promising in process with low return temperatures. A larger temperature glide improved the heat transfer in the condenser. As expected, the COP curves decreased with increasing temperature lift and corresponded to an average Carnot efficiency (2nd Law efficiency) of 39% for R1233zd(E) and 34% for R1336mzz(Z) with the IHX cycle. These values are comparable with the results of Helminger et al. (2016) in another HTHP laboratory setup, but lower than with the commercial HeatBooster technology, which achieves an average efficiency of approx. 41% at 20 kW (Nilsson et al., 2017). The experimental results are promising as the developed HTHP system allows testing alternative HFO and HCFO refrigerants like R1224yd(Z), R1336mzz(E) and R1233zd(E) with stabilizing additives in the future. Temperature-resistant compressors and lubricating oils are decisive components for the further development and commercialization of HTHPs.

ACKNOWLEDGEMENTS

This research project is part of the Swiss Competence Center for Energy Research SCCER EIP of the Swiss Innovation Agency Innosuisse.

NOMENCLATURE

COP	coefficient of performance (–)	Lift	temperature lift from heat source to sink
c_p	specific heat capacity (kJ/kg-K)	ODP	ozone depletion potenial
ΔT	temperature difference (K)	p, T	pressure (bar), temperature (°C)
η_{2nd}	2nd Law efficiency ($\eta_{2nd} = COP_H / COP_{Carnot}$)	P_{el}	electrical power (kW)
GWP_{100}	global warming potential, 100 years	POE	polyolester oil
HCFO	hydrochlorofluoroolefin	$\dot{Q}$	heating capacity (kW)
HFC	hydrofluorocarbon	Ref	reference point conditions
HFO	hydrofluoroolefin	SC, SH	subcooling, superheating

HTHP	high temperature heat pump	SG	safety group classification
IHX	internal heat exchanger	Sink, Source	heat sink, heat source
in, out	inlet, outlet	VHC	Volumetric heating capacity (kJ/m^3)

REFERENCES

AGC Chemicals, 2017. AMOLEA® 1224yd, Technical Information, ASAHI Glass Co., Ltd.

Arpagaus, C., Bless, F., Schiffmann, J., Bertsch, S.S., 2016. Multi-temperature heat pumps: A literature review. Int. J. Refrig. 69, 437–465.

Arpagaus, C., Bless, F., Schiffmann, J., Bertsch, S.S., 2017. Review on High Temperature Heat Pumps – Market Overview and Research Status. In: International Workshop on High Temperature Heat Pumps, September 9, 2017, Copenhagen, Denmark. pp. 1–25.

Arpagaus, C., Bless, F., Uhlmann, M., Büchel, E., Frei, S., Schiffmann, J., Bertsch, S.S., 2018a. High temperature heat pump using HFO and HCFO refrigerants - System design , simulation, and first experimental results. In: 17th International Refrigeration and Air Conditioning Conference at Purdue, July 9-12, 2018. pp. 1–10.

Arpagaus, C., Bless, F., Uhlmann, M., Schiffmann, J., Bertsch, S.S., 2018b. High temperature heat pumps: Market overview, state of the art, research status, refrigerants, and application potentials (Lizenz-/Genehmigungsnummer: 4432121433391). Energy 152, 985–1010.

Arpagaus, C., Bless, F., Uhlmann, M., Schiffmann, J., Bertsch, S.S., 2018c. High temperature heat pumps: Market overview, state of the art, research status, refrigerants, and application potentials. In: 17th International Refrigeration and Air Conditioning Conference at Purdue, July 9-12, 2018. pp. 1–10.

Brown, J.S., Zilio, C., Cavallini, A., 2009. The fluorinated olefin R-1234ze(Z) as a high-temperature heat pumping refrigerant. Int. J. Refrig. 32, 1412–1422.

Fleckl, T., Hartl, M., Helminger, F., Kontomaris, K., Pfaffl, 2015. Performance testing of a lab-scale high temperature heat pump with HFO-1336mzz-Z as the working fluid. In: European Heat Pump Summit 2015, October 20-21, Nuremberg, Germany. pp. 1–25.

Fukuda, S., Kondou, C., Takata, N., Koyama, S., 2014. Low GWP refrigerants R1234ze(E) and R1234ze(Z) for high temperature heat pumps. Int. J. Refrig. 40, 161–173.

Helminger, F., Kontomaris, K., Pfaffl, J., Hartl, M., Fleckl, T., 2016. Measured Performance of a High Temperature Heat Pump with HFO-1336mzz-Z as the Working Fluid. In: ASHRAE 2016 Annual Conference, St. Louis, Missourii, 25-29 June 2016. pp. 1–8.

Kondou, C., Koyama, S., 2015. Thermodynamic assessment of high-temperature heat pumps using low-GWP HFO refrigerants for heat recovery. Int. J. Refrig. 53, 126–141.

Kontomaris, K., 2014a. Zero-ODP, Low-GWP, Nonflammable Working Fluids for High Temperature Heat Pumps. In: ASHRAE Annual Conference, Seattle, Washington, July 1, 2014. pp. 1–40.

Kontomaris, K., 2014b. HFO-1336mzz-Z: High Temperature Chemical Stability and Use as A Working Fluid in Organic Rankine Cycles, Paper 1525. Int. Refrig. Air Cond. Conf. Purdue, July 14-17, 2014.

Myhre, G., Shindell, D., Bréon, F.-M., Collins, W., Fuglestvedt, J., Huang, J., Koch, D., Lamarque, J.-F., Lee, D., Mendoza, B., Nakajima, T., Robock, A., Stephens, G., Takemura, T., Zhang, H., 2013. Anthropogenic and natural radiative forcing. In: Climate Change 2013: The Physical Science Basis. Contribution of Working Group I to the Fifth Assessment Report of the Intergovernmental Panel on Climate Change. Cambridge University Press, Cambridge, United Kingdom and New York, NY, USA, pp. 659–740.

Nilsson, M., Risla, H.N., Kontomaris, K., 2017. Measured performance of a novel high temperature heat pump with HFO-1336mzz-Z as the working fluid. In: 12th IEA Heat Pump Conference 2017, Rotterdam. pp. 1–10.

Patten, K.O., Wuebbles, D.J., 2010. Atmospheric lifetimes and Ozone Depletion Potentials of

trans-1-chloro-3,3,3-trifluoropropylene and trans-1,2-dichloroethylene in a three-dimensional model. Atmos. Chem. Phys. 10, 10867–10874.

Viking Heat Engines, 2018. HeatBooster HBS4: Industrial heat pump for clean energy production up to 160 °C.